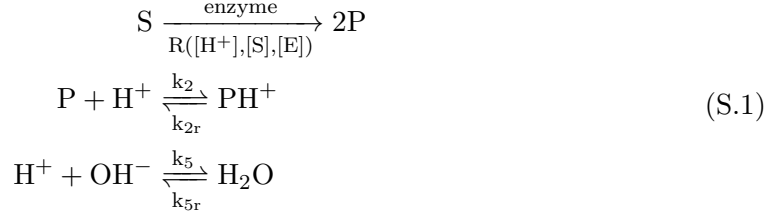


Switches Induced by Quorum Sensing in a Model of Enzyme-loaded
Microparticles
Tamas Bansagi Jr. and Annette F. Taylor
J. R. Soc. Interface

Supplementary Information

Neglecting the production of CO_2 , for it plays a small role in the dynamics, the full mechanism simplifies into



where P , PH^+ and OH^- denote ammonia, ammonium and hydroxide respectively. The corresponding reaction-diffusion equations in one spatial dimension are

$$\partial_t[\text{S}] = D_S \partial_x^2[\text{S}] - \text{R} \quad (\text{S.2a})$$

$$\partial_t[\text{P}] = D_P \partial_x^2[\text{P}] + 2\text{R} - k_2[\text{P}][\text{H}^+] + k_{2r}[\text{PH}^+] \quad (\text{S.2b})$$

$$\partial_t[\text{PH}^+] = D_{\text{PH}} \partial_x^2[\text{PH}^+] + k_2[\text{P}][\text{H}^+] - k_{2r}[\text{PH}^+] \quad (\text{S.2c})$$

$$\partial_t[\text{H}^+] = D_H \partial_x^2[\text{H}^+] + k_{5r} - k_5[\text{H}^+][\text{OH}^-] + k_{2r}[\text{PH}^+] - k_2[\text{P}][\text{H}^+] \quad (\text{S.2d})$$

$$\partial_t[\text{OH}^-] = D_{\text{OH}} \partial_x^2[\text{OH}^-] + k_{5r} - k_5[\text{H}^+][\text{OH}^-]. \quad (\text{S.2e})$$

The equilibrium between H_2O , H^+ and OH^- is assumed to be established instantaneously, therefore $[\text{OH}^-]$ can be substituted with $K_w/[\text{H}^+]$ in eq. (S.2e) converting the LHS into

$$\partial_t[\text{OH}^-] = \frac{d(K_w/[\text{H}^+])}{d[\text{H}^+]} \partial_t[\text{H}^+] = -\frac{K_w}{[\text{H}^+]^2} \partial_t[\text{H}^+].$$

Subtracting eq. (S.2e) from eq. (S.2d) and, for convenience, assuming that $D_H = D_{\text{OH}}$ as well as using the linearity of differentiation ($D_H \partial_x^2[\text{H}^+] - D_{\text{OH}} \partial_x^2(K_w/[\text{H}^+]) = D_H \partial_x^2([\text{H}^+] - K_w/[\text{H}^+])$) yields:

$$\left(1 + \frac{K_w}{[\text{H}^+]^2}\right) \partial_t[\text{H}^+] = D_H \partial_x^2 \left([\text{H}^+] - \frac{K_w}{[\text{H}^+]}\right) + k_{2r}[\text{PH}^+] - k_2[\text{P}][\text{H}^+] \quad (\text{S.3})$$

Figure 1 shows the rate terms ($2\text{R} - k_2[\text{P}][\text{H}^+] + k_{2r}[\text{PH}^+]$) and ($-k_2[\text{P}][\text{H}^+] + k_{2r}[\text{PH}^+]$) during a cycle. It can be seen that $2\text{R} - k_2[\text{P}][\text{H}^+] + k_{2r}[\text{PH}^+] \approx 0$ for the acidic part of a cycle where autocatalysis occurs (Figure 1a, solid line), and that $-k_2[\text{P}][\text{H}^+] + k_{2r}[\text{PH}^+] \approx 0$ for the remainder (Figure 1a, dashed line). Using the latter assumption to reduce the model removes the feedback mechanism and results in the loss of oscillations. Hence, we substitute ($-k_2[\text{P}][\text{H}^+] + k_{2r}[\text{PH}^+]$) with -2R in eq. (S.3) on the basis that this simplification alters the dynamics only moderately. As a result eq. (S.2) reduces into the 2-variable model:

$$\begin{aligned} \partial_t[\text{S}] &= D_S \partial_x^2[\text{S}] - \text{R} \\ \partial_t[\text{H}^+] &= \left[D_H \partial_x^2 \left([\text{H}^+] - \frac{K_w}{[\text{H}^+]}\right) - 2\text{R} \right] \left(1 + \frac{K_w}{[\text{H}^+]^2}\right)^{-1}. \end{aligned} \quad (\text{S.4})$$

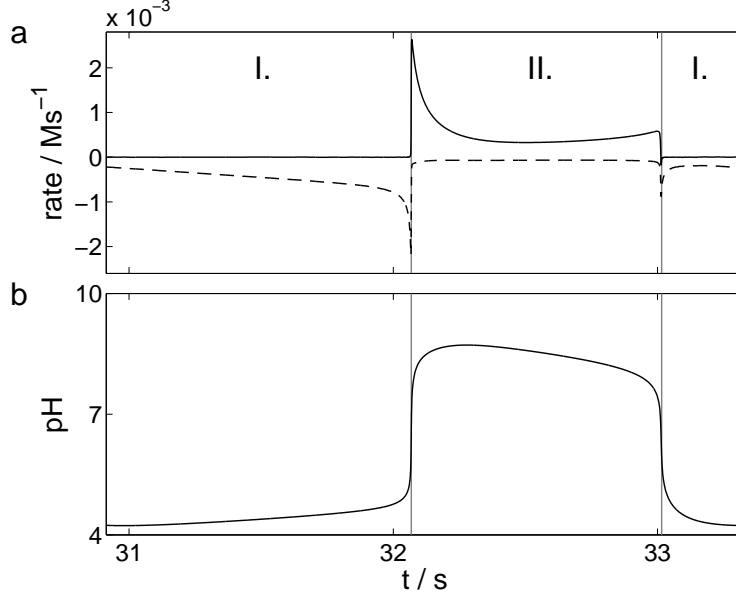


Figure 1: Comparison of rates during a single oscillation in the five-variable model: (a) solid line: $2R - k_2[P][H^+] + k_{2r}[PH^+]$; dashed line: $-k_2[P][H^+] + k_{2r}[PH^+]$. (b) pH. Gray lines mark the boundary between the acidic (I.) and basic (II.) parts of a cycle. Parameters as in fig. 2.

pH traces for the five- and two-variable models are shown in Figure 2. The reduced model captures the main characteristics of the oscillatory cycle reasonably well, *i.e.* the period and amplitude.

Introducing $s = [S]/K_m$, $h = [H^+]/K_{ES1}$, $d = D_H/D_S$, $\kappa = K_m/K_{ES1}$, $\kappa_{es} = K_{ES2}/K_{ES1}$, $\kappa_w = K_w/K_{ES1}^2$, $\tau = t k_E[E]/K_m$, $x' = x(k_E[E])^{1/2}(D_S K_m)^{-1/2}$, where τ and x' are dimensionless time and space, respectively; the one-dimensional spatial model corresponding to eq. (S.4) becomes:

$$\begin{aligned} \partial_\tau s &= \partial_{x'}^2 s - r \\ \partial_\tau h &= \left[d \partial_{x'}^2 \left(h - \frac{\kappa_w}{h} \right) - 2\kappa r \right] \left(1 + \frac{\kappa_w}{h^2} \right)^{-1} \end{aligned} \quad (S.5)$$

where

$$r = \frac{s}{(1+s)(1+\kappa_{es}/h+h)}.$$

In three-dimensions, diffusive transport is considered through applying the $\nabla^2 = (\partial_x^2 + \partial_y^2 + \partial_z^2)$ Laplace operator to the concentration field of chemical components. The finite difference form of the Laplacian is chosen depending on the spatial geometry of the studied system. Having enzyme-loaded beads in a 2D hexagonal lattice within a 3D volume lends itself to resolving the entire space as a hexagonal-close-packed (*hcp*) array of cells (Figure 3a). To approximate the diffusion-induced concentration change with time inside each cell, we define vectors $\vec{u}_i = (u_{i,x}, u_{i,y}, u_{i,z})$ pointing from the center of a cell to the center of the adjacent cells, with $|\vec{u}_i| = 1$ being the grid spacing (Figure 3b). The $D_{\vec{u}} f|_{f_0}$ and $D_{\vec{u}}^2 f|_{f_0}$ directional first and second derivatives of f at f_0 along $\vec{f}_0 \vec{f}_i$ are computed (after dropping i) according to

$$D_{\vec{u}} f = (u_x, u_y, u_z) \cdot (\partial_x f, \partial_y f, \partial_z f) = u_x \partial_x f + u_y \partial_y f + u_z \partial_z f,$$

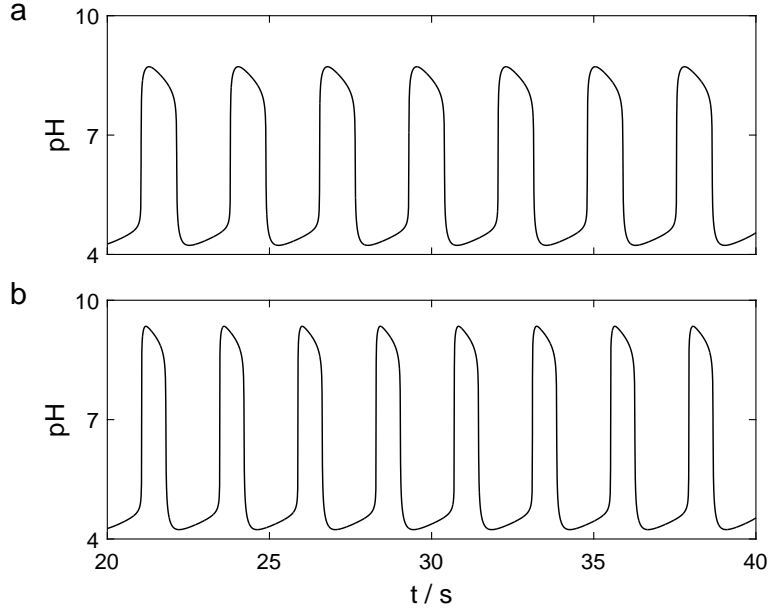


Figure 2: pH oscillations in the middle of a $100 \mu\text{m}$ wide, urease-loaded ($E = 12000 \text{ u/ml}$) 1D compartment in contact with acidic urea solution ($[S]_0 = 0.35 \text{ mM}$; $[H^+]_0 = 0.1 \text{ mM}$) in the (a) five-variable model: eq. (S.2); and (b) two-variable model: eq. (S.4). In the five-variable model $D_S = D_P = D_{PH} = 1.4 \times 10^{-5} \text{ cm}^2 \text{ s}^{-1}$; $D_H = 9 \times 10^{-5} \text{ cm}^2 \text{ s}^{-1}$; $D_{OH} = 6 \times 10^{-5} \text{ cm}^2 \text{ s}^{-1}$.

$$D_{\vec{u}}^2 f = D_{\vec{u}}(D_{\vec{u}} f) = u_x^2 \partial_x^2 f + u_y^2 \partial_y^2 f + u_z^2 \partial_z^2 f + 2u_x u_y \partial_{xy}^2 f + 2u_x u_z \partial_{xz}^2 f + 2u_y u_z \partial_{yz}^2 f$$

which, in turn, can be used in estimating f_i via Taylor-expansion as

$$f_i \approx f_0 + l D_{\vec{u}_i} f|_{f_0} + \frac{l^2}{2} D_{\vec{u}_i}^2 f|_{f_0}.$$

By realizing that the first and mixed second partial derivatives cancel out (coefficients for

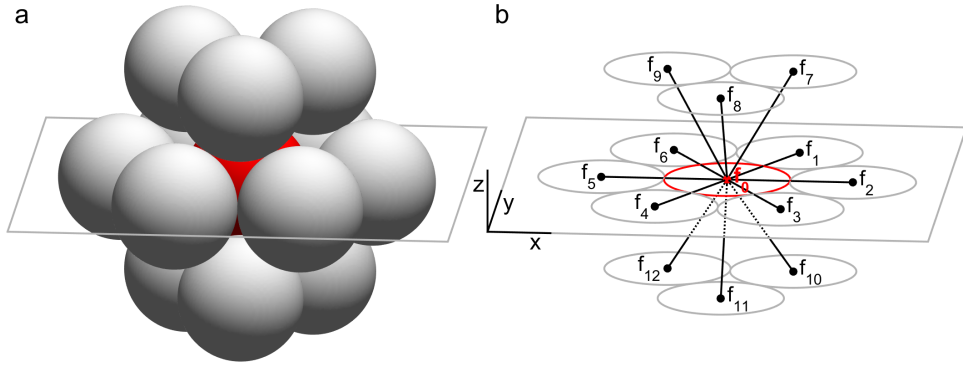


Figure 3: Unit cell configuration of hexagonal close-packed grid. f denotes $f(x, y, z)$, whereas f_0 and f_i stand for $f(x_0, y_0, z_0)$ and $f(x_i, y_i, z_i)$, respectively at the same instant in time.

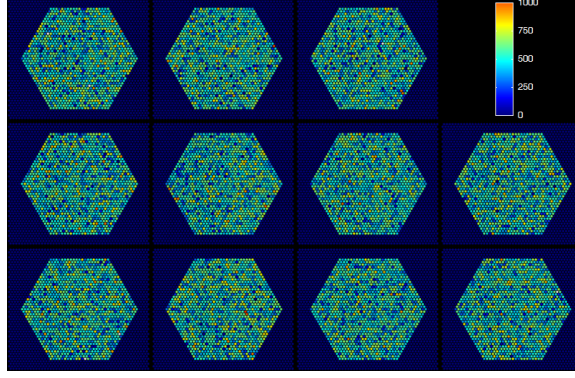


Figure 4: Spatial distributions of enzyme with mean 500 and standard deviation 150 ($\mu = 1$, $\sigma = 0.3$) within arrays of beads.

the partial derivatives are listed in Table 1), we find that

$$\sum f_i \approx 12f_0 + 2l^2(\partial_x^2 f|_{f_0} + \partial_y^2 f|_{f_0} + \partial_z^2 f|_{f_0}),$$

thus for a grid node representing a cell in an *hcp* lattice the Laplacian can be approximated as

$$\nabla_{hcp}^2 f_0 \approx \frac{\sum f_i - 12f_0}{2l^2}. \quad (\text{S.6})$$

Spatial inhomogeneity in enzyme was implemented though multiplying the rate term for each microbead with a coefficient. Coefficient values were generated using the Marsaglia–Bray method [S1] and followed the normal distribution with mean (μ) equal to one and standard deviations (σ): 0.1, 0.2 and 0.3.

i	u_x	u_y	u_z
1	1/2	$\sqrt{3}/2$	0
2	1	0	0
3	1/2	$-\sqrt{3}/2$	0
4	-1/2	$-\sqrt{3}/2$	0
5	-1	0	0
6	-1/2	$\sqrt{3}/2$	0
7	1/2	$\sqrt{3}/6$	$\sqrt{6}/3$
8	0	$-\sqrt{3}/3$	$\sqrt{6}/3$
9	-1/2	$\sqrt{3}/6$	$\sqrt{6}/3$
10	1/2	$\sqrt{3}/6$	$-\sqrt{6}/3$
11	0	$-\sqrt{3}/3$	$-\sqrt{6}/3$
12	-1/2	$\sqrt{3}/6$	$-\sqrt{6}/3$

Table 1: Coefficients for partial derivatives in $D_{\vec{u}} f|_{f_0}$ and $D_{\vec{u}}^2 f|_{f_0}$.

References

- [S1] G. Marsaglia and T.A. Bray, *A convenient method for generating normal variables*, SIAM Review, 6, 260, 1964